

Evaluation of the shear frame test for weak snowpack layers

BRUCE JAMIESON, COLIN D. JOHNSTON

Department of Civil Engineering, University of Calgary, 2500 University Drive NW, Calgary, Alberta T2N 1N4, Canada

ABSTRACT. The shear frame allows testing of thin weak snowpack layers that are often critical for slab avalanche release. A shear metal frame with an area of 0.01–0.05 m² is used to grip the snow a few mm above a buried weak snowpack layer. Using a force gauge, the frame is pulled until a fracture occurs in the weak layer within 1 s. The strength is calculated from the maximum force divided by the area of the frame. Finite-element studies show that the shear stress in the weak layer is concentrated below the cross-members that subdivide the frame and where the weak layer is notched at the front and back of the frame. Placing the bottom of the frame in the weak layer increases the stress concentrations, and results in significantly lower strength measurements than placing the bottom of the frame a few mm above the weak layer. Based on over 800 sets of 7–12 tests in western Canada, coefficients of variation average 14% and 18% from level study plots and avalanche start zones, respectively. Consequently, sets of 12 tests typically yield a precision of the mean of 10% with 95% confidence, which is sufficient for monitoring of strength change of weak layers over time in study plots. With consistent technique, there is no significant difference in mean strength measurements obtained by different experienced shear frame operators using the same approximate loading rate and technique for placing the frame. Although fracture surfaces are usually planar, only one of eleven shapes of non-planar fracture surfaces showed significantly different strength compared to planar fracture surfaces. For weak layers thick enough for density measurements, the shear strength is plotted against density and grain form. From these data, empirical equations are determined to estimate the shear strength of weak snowpack layers.

INTRODUCTION

The shear strength of thin weak snowpack layers is critical for slab avalanche release. Since snowpack specimens that include these thin weak layers cannot be transported to a cold laboratory without disturbance, in situ shear frame tests are presently the only practical way to measure the shear strength of such layers and to monitor their strength over time. The rotary shear vane similar to that used for testing soils has been used to test *homogeneous* snow layers (Keeler and Weeks, 1968; Martinelli, 1971; Perla and others, 1982; Brun and Rey, 1987) but cannot be positioned with sufficient accuracy for testing thin weak snowpack layers.

For the shear frame test, a shear metal frame with an area of 0.01–0.05 m² is used to grip the snow a few mm above a buried weak snowpack layer (Fig. 1). Using a force gauge, the frame is pulled quickly, producing a brittle fracture in the underlying weak layer. The shear strength, Σ , is calculated from the maximum force divided by the area of the frame.

In addition to the shear strength of the layer being tested, the results of shear frame tests may also be affected by or related to various test factors. This study analyzes the effect of different operators, the shape of the fracture surface, and the distance between the bottom of the frame and the weak layer. Since the operator may refine the manual loading rate or the frame placement while repeatedly testing the same layer, the test sequence may also affect the results. To facilitate the statistical analyses of these factors, most repeated shear strength measurements are shown to be normally distributed. Also, based on a compilation of the shear frame measurements, the dependence of shear strength of weak snowpack layers on grain form and density is studied.

LITERATURE REVIEW

The shear frame test was developed by A. Roch about 1950 (De Quervain, 1951). It has been used for avalanche research since 1966 (Roch, 1966a, b) and for avalanche forecasting since 1962 (Schleiss and Schleiss, 1970).



Fig. 1. Photograph of shear frame being pulled. Weak layer is a few mm below the bottom of the frame.

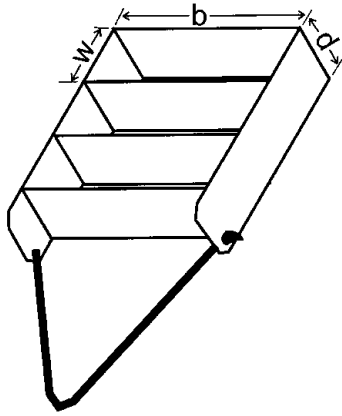


Fig. 2. Diagram of 0.025 m^2 shear frame recommended by Sommerfeld (1984) and used in present study and previous studies by Sommerfeld and others (1976), Sommerfeld and King (1979) and Perla and Beck (1983).

For shear frame tests of snowpack layers, the load is applied manually with a force gauge that records the maximum force. Perla and Beck (1983) found the strength was reduced by 25% when loading times were reduced from approximately 30 s to approximately 3 s. Jamieson (1995) found the effect of loading rate on strength measurements was reduced for loading times of < 1 s and was negligible for mean strengths of < 1 kPa. However, Föhn and Camponovo (1997) found that the percentage of planar fracture surfaces was increased if frames were pulled to failure within 2.5 s rather than within 1 s. Using a displacement sensor and accelerometer with a shear frame, Föhn and others (1998) found approximately linear stress–strain behaviour and shear strain rates between 10^{-2} s^{-1} and 1 s^{-1} . This is well within the range observed for brittle fractures of depth hoar in shear tests (Fukuzawa and Narita, 1993) and for brittle tensile tests of decomposed and fragmented particles (Singh, 1980) or rounded grains (Narita, 1980; Singh, 1980).

Sommerfeld (1973), Sommerfeld and others (1976) and Sommerfeld and King (1979) proposed that size effects in shear frame tests could be explained by Daniels' (1945) thread bundle statistics. Gubler (1978) questioned the use of Daniels' statistics for rapid loading which does not permit stress redistribution after part of the specimen has fractured. However, Sommerfeld (1980) showed that the ratio of mean strengths with different sizes of frames agrees with the ratios predicted by Daniels' statistics. Föhn (1987b) compiled his results with those of Perla (1977) and Sommerfeld (1980) to obtain a curve of correction factors. For frames larger than 0.3 m^2 , mean shear strengths asymptotically approached the strength of an arbitrarily large specimen. This asymptote, denoted Σ_{∞} in the present study, can be obtained by multiplying the mean strength obtained with a particular area of frame by the appropriate correction factor. For frames with areas of 0.01, 0.025 and 0.05 m^2 , the correction factors are 0.56, 0.65 and 0.71, respectively (Sommerfeld, 1980; Föhn, 1987b).

To distribute the applied stress more evenly through the snow layer being tested, Roch's (1966a, b) frames had two intermediate cross-members (fins). The relatively rigid outer frame distributes the manually applied load equally onto the rear cross-member and the two intermediate cross-members. The lower tip of each of these *active* cross-members creates a shear stress concentration in the weak snow layer. These stress concentrations are influenced by the ratio of the height of the cross-member, d , to the length of the snow sub-specimen in

front of the cross-member, w (Fig. 2). Perla and Beck (1983) suggested that by decreasing the d/w ratio, the stress concentration at the lower tip of the cross-member is increased, and that increasing d/w will increase the normal load and may contribute to increased disturbance of the weak layer when the frame is inserted.

Roch's (1966b) 0.01 m^2 frame had three active cross-members and a d/w ratio of 3:4. The present study used the frame design (Fig. 2) preferred by Perla and Beck (1983) and Sommerfeld (1984) which had an area of 0.025 m^2 , $d = 40 \text{ mm}$, $w = 53 \text{ mm}$, three active cross-members and a slightly trapezoidal shape ($b = 154\text{--}164 \text{ mm}$) to minimize friction between the frame and the snow on either side. If constructed of 0.6 mm stainless steel with soldered joints, a frame with these dimensions has a mass of approximately 0.2 kg.

TEST METHOD

Before the shear frame test is performed, the weak layer is identified by a snow profile (e.g. CAA, 1995), a tilt board test, a shovel test or a rutschblock test (Föhn, 1987a). Overlying snow is removed, leaving approximately 40–45 mm of undisturbed snow above the weak layer (Fig. 1). The shear frame, constructed of 0.6 mm stainless steel with sharpened lower edges, is then gently inserted into the undisturbed snow so that the bottom of the frame is usually within 2–5 mm of the weak layer (Perla and Beck, 1983). In practice, the strengths of the weak layer and the snow above the weak layer (the superstratum) influence the distance between the weak layer and the bottom of the frame. If the superstratum is not much harder than the weak layer, then the shear frame must often be placed very close to, or into, the weak layer to avoid a fracture in the superstratum rather than in the weak layer when the frame is pulled. Alternatively, if the superstratum is very hard, then the weak layer may fracture during frame placement. Under such conditions, frames must be placed 5–10 mm above the weak layer and occasionally higher. The effect of frame placement more or less than the recommended 2–5 mm is discussed subsequently. After the frame is placed, a thin blade is passed around the sides of the frame to ensure that surrounding snow is not in contact with, and possibly bonding to, the frame. This cut must extend to the weak layer to ensure that a known area is tested, but not through the weak layer to avoid notching the layer below (substratum). The force gauge is attached to the cord linking the two sides of the frame and is pulled smoothly and quickly (< 1 s), usually resulting in a planar failure in the weak layer just below the base of the frame. Tests in which half or more of the fracture surface deviated beyond the active weak layer are rejected.

For two people working as operator and recorder to make 12 shear frame tests, about 30 min is required, plus the time required to dig the pit.

SHEAR STRESS IN WEAK LAYER INDUCED BY SHEAR FRAME

We used a finite-element model to determine the shear stress distribution in the weak layer caused by shear frame tests and to qualitatively assess the effect on the stress distribution due to the proximity of the shear frame to the weak layer.

The basic geometry of the model is shown in Figure 3. The models consist of three isotropic homogeneous layers: the snow within the frame (superstratum), the weak layer and

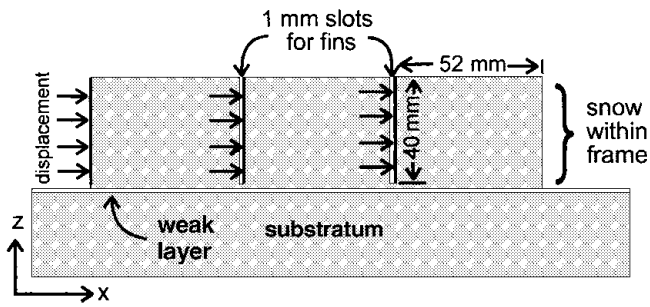


Fig. 3. Geometry and loading for finite-element model of standard shear frame placed 3 mm above weak layer.

Table 1. Material properties for finite-element model

Layer	Nominal density kg m ⁻³	Young's modulus MPa	Poisson's ratio
Superstratum	200	1	0.25
Weak layer	160	0.2	0.25
Bed surface	200	1	0.25

Table 2. Finite-element models of the shear frame test

Model name	Shear frame	Frame placement with respect to weak layer	Number of elements	Displacement necessary for average shear stress of 1 kPa mm
std-ab-soft	std	3 mm above	7130	0.130
std-in-soft	std	1 mm into	6604	0.130

the bed surface (substratum). The superstratum is modelled as part of a soft slab (~200 kg m⁻³). The weak layer is modelled as a 2 mm thick softer layer (~160 kg m⁻³). Material properties for the three layers were chosen from Mellor's (1975) compilation of snow properties and are shown in Table 1. In the first model (std-ab-soft in Table 2) the bottom of the frame is 3 mm above the weak layer. In the second model (std-in-soft), the bottom of the frame is 1 mm into the 2 mm thick weak layer.

The substratum is fixed 30 mm to the right of the frame, 20 mm to the left of the frame, and at the base 30 mm below the weak layer. Since the frame is relatively rigid compared to the snow being tested, a constant displacement to the right is applied to the left surfaces of the snow within the frame. This displacement loading is in preference to pressure loading which would tend to tilt the snow in the compartments unrealistically. The displacement is chosen to cause an average shear stress in the weak layer of 1.0 kPa which is typical of the shear strength of a weak snow layer (Table 2).

A linear model is used since shear frame loading times (<1s) are well within the range associated with linear stress-strain curves and brittle failures for tension (Narita, 1980; Singh, 1980) and for shear (Fukuzawa and Narita, 1993). However, such macroscopic linear behaviour does not rule out small-scale plasticity at stress concentrations and grain boundaries. Nevertheless, linear elasticity is assumed since it is sufficient to provide qualitative compar-

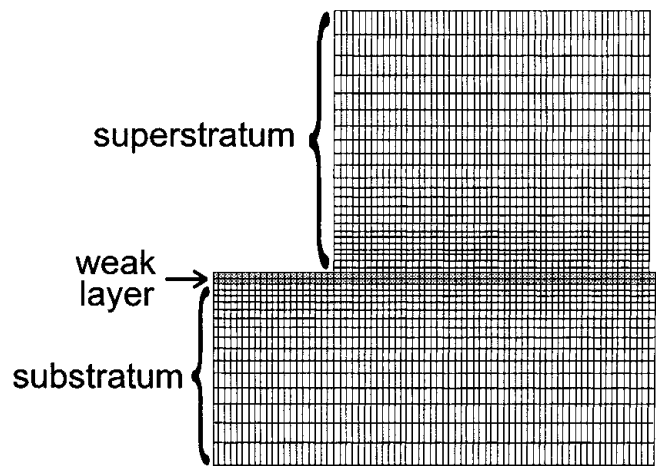


Fig. 4. Mesh of elements for snow in left compartment and underlying weak layer and substratum.

isons of frame placements and material properties. Since the sides of the frame restrict expansion during loading, a two-dimensional plane strain model is used.

Each element is a bilinear quadrilateral with nodes at each corner and the midpoint of each of the four sides. Such elements have a quadratic shape function which allows the sides of the elements to curve during deformation. In and near the lower tips of the active cross-members and the weak layer, the elements are 1 mm by 1 mm prior to loading as shown in Figure 4. At the upper and lower surfaces of the model, well away from the weak layer, the size of the elements increases to 4 mm by 1 mm to reduce the number of elements and consequently the number of computations. Elements are joined at nodes, providing continuity. Boundary conditions, such as displacements, are applied at the nodes. As a consequence of the assumed linear elasticity, the peak stresses depend strongly on the size of the elements, with smaller elements resulting in higher peak stresses. The same mesh of elements in and near the weak layer is used for both models. Thus, the peak stresses reflect, at least relatively, the frame placement. The models, material properties and boundary conditions were encoded using Patran software. Finite-element calculations were done by Abaqus software.

The contour plot of σ_{xz} shows a stress concentration at each of the three active cross-members plus one at the right cross-member (Fig. 5). This rightmost stress concentration indicates the effect of cutting around the frame with a blade through the 3 mm of superstratum below the frame and into the weak layer. The stress concentration at the leftmost cross-member is partly due to the applied displacement

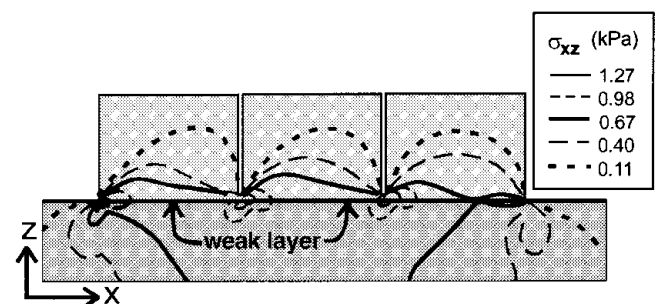


Fig. 5. Contours for shear stress, σ_{xz} , in snow for standard frame placed in soft superstratum 3 mm above weak layer.

and partly due to the notching of the weak layer by the blade. The superposition of these two stress concentrations results in the peak stress near the leftmost (back) cross-member (Fig. 5). The stress concentration at the bottom of each of the three active cross-members has two lobes. These two lobes extend into the weak layer which is 3 mm below the bottom of the cross-members and can be seen as peaks in σ_{XZ} as shown in Figure 5.

EFFECT OF FRAME PLACEMENT ON SHEAR DISTRIBUTION

Typically, the shear frame is placed in the superstratum so that the bottom of the shear frame is 2–5 mm above the top of the weak layer. However, in practice the distance necessary to achieve planar shear failures ranges between 0 and 20 mm depending on the strength of the weak layer and the hardness of the layer above the weak layer. As shown in Figure 6, the peak values of σ_{XZ} are reduced when the frame is placed 3 mm above the 2 mm thick weak layer compared to frame placements 1 mm into the 2 mm thick weak layer. This is consistent with experimental results discussed subsequently. The analysis confirms that the more uniform stress distribution when the frame is placed above the weak layer is advantageous and should be used whenever practical.

STATISTICAL DISTRIBUTION OF REPEATED STRENGTH MEASUREMENTS

Strengths determined from shear frame tests can be consid-

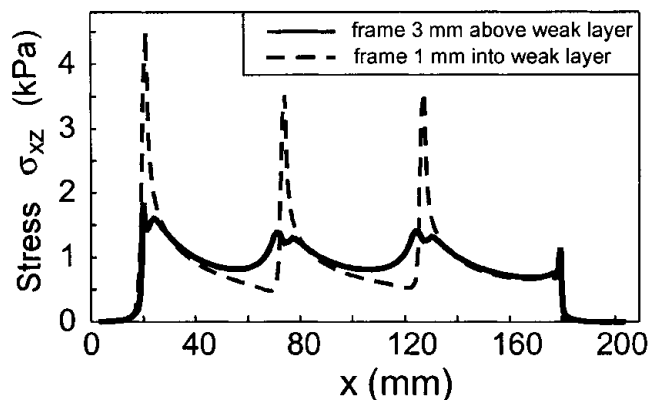


Fig. 6. Shear stress, σ_{XZ} , in weak layer below frame when frame is placed 1 mm into a 2 mm thick weak layer and 3 mm above a 2 mm thick weak layer.

ered continuous, and certainly they have the properties of interval data. Analyses of such data are facilitated if the data are normally distributed. To assess the normality of shear frame results, 28 sets of 30 or more tests with standard frames from the winters of 1991–95 are summarized in Table 3. The normality of these data was assessed with the chi-squared (χ^2) and Kolmogorov–Smirnov (d statistic) goodness-of-fit tests. For the chi-squared test, cells are combined so that there are at least five data in each cell and each of the 28 sets of 30–38 data was partitioned into five cells. The χ^2 statistic as well as the degrees of freedom df and p are given in Table 3. There are five sets in which $p < 0.05$, implying a $< 5\%$ probability

Table 3. Goodness-of-fit tests for large sets of shear strength measurements

Date	Grain form (of most common grains in weak layer)	Mean strength kPa	Coef. of var. V	Number of tests n	Kolmogorov–Smirnov test			Chi-squared test		
					d	p	Lilliefors p	df	χ^2	p
19 Dec. 1991	Decomp. & frag.	0.301	0.167	30	0.184	<0.20	<0.01	2	7.76	0.02
20 Dec. 1991	Precip. particles	0.345	0.100	36	0.077	n.s.	n.s.	2	2.18	0.34
21 Dec. 1991	Decomp. & frag.	0.525	0.084	32	0.210	<0.10	<0.01	2	1.04	0.59
11 Feb. 1992	Decomp. & frag.	1.096	0.108	38	0.173	n.s.	<0.01	2	9.70	0.01
14 Feb. 1992	Surface hoar	0.386	0.083	30	0.189	n.s.	<0.01	2	11.7	10⁻³
17 Feb. 1992	Surface hoar	0.645	0.129	30	0.119	n.s.	n.s.	2	4.40	0.11
10 Apr. 1992	Facets	0.614	0.195	32	0.102	n.s.	n.s.	2	0.84	0.66
6 Feb. 1993	Surface hoar	2.129	0.199	32	0.090	n.s.	n.s.	2	1.66	0.44
13 Feb. 1993	Surface hoar	3.181	0.144	32	0.124	n.s.	n.s.	2	3.62	0.16
24 Feb. 1993	Surface hoar	0.476	0.141	32	0.124	n.s.	n.s.	2	0.67	0.72
3 Mar. 1993	Surface hoar	0.615	0.147	30	0.127	n.s.	n.s.	2	1.82	0.40
16 Mar. 1993	Facets	2.157	0.172	31	0.112	n.s.	n.s.	2	3.72	0.16
1 Apr. 1993	Facets	2.208	0.179	30	0.122	n.s.	n.s.	2	4.22	0.12
30 Mar. 1994	Graupel	4.013	0.123	30	0.126	n.s.	n.s.	2	2.93	0.23
4 Dec. 1994	Graupel	0.931	0.135	30	0.111	n.s.	n.s.	2	0.84	0.66
15 Dec. 1994	Decomp. & frag.	0.219	0.135	30	0.208	<0.15	<0.01	2	13.5	10⁻³
29 Dec. 1994	Graupel	1.432	0.197	30	0.146	n.s.	<0.10	2	4.59	0.10
4 Jan. 1995	Graupel	2.124	0.160	30	0.117	n.s.	n.s.	2	2.62	0.27
29 Jan. 1995	Surface hoar	1.294	0.199	30	0.193	<0.20	<0.01	2	1.74	0.42
9 Feb. 1995	Surface hoar	3.710	0.090	33	0.194	<0.15	<0.01	2	4.04	0.13
22 Feb. 1995	Surface hoar	1.874	0.118	30	0.149	n.s.	<0.10	2	1.92	0.38
28 Feb. 1995	Surface hoar	3.035	0.083	36	0.144	n.s.	<0.10	2	2.66	0.27
7 Mar. 1995	Surface hoar	4.185	0.075	30	0.096	n.s.	n.s.	2	2.66	0.27
24 Mar. 1995	Graupel	2.764	0.150	30	0.176	n.s.	<0.05	2	3.27	0.19
28 Mar. 1995	Graupel	3.597	0.100	30	0.076	n.s.	n.s.	2	4.22	0.12
29 Mar. 1995	Surface hoar	5.921	0.090	30	0.130	n.s.	n.s.	2	5.94	0.05
23 Jan. 1995	Surface hoar	4.139	0.097	30	0.130	n.s.	n.s.	2	1.43	0.49
29 Jan. 1995	Surface hoar	1.204	0.109	33	0.118	n.s.	n.s.	2	3.00	0.22

Notes: Significance levels < 0.05 are marked in bold; n.s., not significant.

that the set came from normally distributed data. However, because the results of chi-squared tests depend on the choice of cell boundaries, the results of Kolmogorov–Smirnov tests are also included in Table 3. Since the normal parameters are calculated from the sets prior to fitting, we use the Lilliefors p in preference to the Kolmogorov–Smirnov p for assessing the d statistic (Statsoft, 1994, p. 1379). As indicated in Table 3, only the range of these significance levels (e.g. < 0.05) can be calculated. There are eight sets for which the Lilliefors $p < 0.05$, and for four of these sets chi-squared $p < 0.05$. Notably, all four sets of strength measurements for decomposed and fragmented particles fail one or both of the goodness-of-fit tests. Since the hypothesis of normality cannot be rejected for 20 (Lilliefors $p < 0.05$) to 24 (chi-squared $p < 0.05$) of the 28 datasets, the shear frame data are assumed to be normally distributed. However, further studies of decomposed and fragmented precipitation particles would be worthwhile.

VARIABILITY AND NUMBER OF TESTS FOR REQUIRED PRECISION

The spatial variability of shear strength of a particular weak layer throughout an area such as an avalanche start zone is certainly relevant to stability evaluation, but digging numerous pits in every start zone or study plot of concern requires too much time for any avalanche-forecasting operation. Safety concerns also limit access to avalanche start zones. Hence, the variability reported for the present studies and for previous studies (except for Sommerfeld and King, 1979) is for repeated shear frame tests of a particular weak layer *in a single pit*, usually within 30–60 min. Shear frame tests are usually made in one or two rows across the slope, and the area tested by 7–12 shear frame tests is usually < 0.5 m by 2 m.

The coefficient of variation is the preferred measure of variability for snow strength since it is less dependent on mean strength than the standard deviation which increases with mean strength (Keeler and Weeks, 1968; Jamieson, 1989). Previously reported coefficients of variation for 0.01, 0.025 and 0.05 m² shear frame tests are typically 0.25 but range from 0.18 to 0.62 (Perla, 1977; Sommerfeld and King, 1979; Föhn, 1987b; personal communication from P. Schaerer, 1991). The highest values of 0.54, 0.52 and 0.62 were reported by Sommerfeld and King (1979) who tested the failure plane at up to three sites along crown fractures.

During the winters of 1989/90 to 1994/95, 809 sets of six or

more shear frame tests (with areas of 0.01, 0.025 or 0.05 m²) were made in study sites chosen partly for uniformity of snowpack, and in avalanche start zones where greater variability is expected. For these 809 sets, the coefficients of variation ranged from 0.03 to 0.66 with a mean of 0.152. At level study plots (inclination $< 3^\circ$) chosen for a uniform snowpack, the coefficients of variation from 342 sets of six or more tests ranged from 0.03 to 0.46 with a mean of 0.144. In avalanche start zones with inclinations of at least 35° , the coefficients of variation from 114 sets of six or more tests ranged from 0.04 to 0.54 with a mean of 0.178. The remaining 353 sets are from sites, mainly study slopes, with slope inclinations of 3 – 34° .

The present study's coefficients of variation are generally lower than those from previous studies. This may be due to reduced disturbance of the weak layer due to the use of shear frames constructed of relatively thin stainless steel with sharpened lower edges, consistently fast loading resulting in fractures within 1 s, the generally consistent snowpack of the Columbia Mountains, Canada, where most of the tests were done, or the field practice of rejecting tests that do not fail on the intended layer or that show definite evidence of disturbance, such as pine needles or an animal track in the fracture surface. (Test results were *not* rejected due to surprisingly low or high pull forces.)

To determine the number of tests n required to obtain precision P with confidence $1 - 2\alpha$, we use a two-tailed t -test

$$t_{\alpha;n-1} = \frac{|\bar{X} - \mu|\sqrt{n}}{s}, \quad (1)$$

where μ is the population mean, \bar{X} is the sample mean and s is the sample standard deviation.

Since the coefficient of variation is $V = s/\bar{X}$ and the precision is $P = |\bar{X} - \mu|/\bar{X}$, we rewrite Equation (1) as

$$t_{\alpha;n-1} = \frac{P\sqrt{n}}{V} \quad (2)$$

and solve for n .

For $V = 0.15$ which is typical of study plots in the present study, eight tests are required for a precision of 10% with 90% confidence. Twelve tests yield a precision of 8% with 90% confidence or a precision of 10% with 95% confidence. The reduced variability from the present study results in fewer tests being necessary to achieve a chosen level of precision. This is an important point for avalanche safety operations because a greater number of tests would require a larger pit and more time, and could be operationally impractical.

Table 4. Assessment of common shapes of fracture surfaces

Descriptor	Description of fracture surface	n	Sample		t-test	
			Mean	Std dev.	t	p
C	Smooth, planar	5757	-0.02	0.95	-	-
SBD	Divot under rear compartment, divot < 5 mm deep	200	0.02	0.93	-0.66	0.51
MBD	Divot under rear compartment, divot 5–10 mm deep	154	0.09	0.90	-1.46	0.15
BBD	Divot under rear compartment, divot > 10 mm deep	131	0.41	0.93	-5.19	7E-07
W	One wave per compartment, waves 5–10 mm deep	243	0.01	0.94	-0.54	0.59
SW	One wave per compartment, waves < 5 mm deep	77	0.03	0.85	-0.54	0.59
SIR	Irregularities < 5 mm deep	44	0.13	0.9	-1.09	0.28
IRR	Irregularities 5–10 mm deep	114	0.10	0.96	-1.28	0.20
LC	Fractured deeper at right or left side	31	0.27	0.87	-1.84	0.07
SH	Small hump, height < 5 mm	22	-0.25	1.04	1.04	0.31
STP	Stepped between two fracture planes	21	0.31	0.94	-1.60	0.12
BC	Back divot extends beyond rear compartment	14	-0.11	1.30	0.26	0.80

Note: Row for which $p < 0.05$ is marked in bold.

Table 5. Effect of test sequence on the standard deviation

Sequence No.	Number of tests in set	Mean	Std dev.
1	703	-0.004	1.111
2	703	-0.008	0.985
3	702	0.007	0.903
4	701	0.06	0.943
5	696	0.001	0.91
6	691	0.048	0.92
7	674	0.005	0.93
3-7	3464	0.024	0.921

FRACTURE SURFACE

During the winters of 1991-95, 703 sets of shear frame tests were made with standard 0.025 m² frames for a total of 8468 tests. The shapes of the fracture surfaces were classified with the standard descriptors (Table 4) for 6951 tests, and 5757 of these (83%) exhibited smooth planar fracture surfaces. Shapes that occurred <10 times are excluded from Table 4 and this analysis.

To compare the strength measurements associated with planar fracture surfaces with measurements associated with other shapes of fracture surfaces, each strength, Σ_{*i*}, was converted to standard normal

$$X_i = \frac{(\Sigma_i - \bar{\Sigma})}{s_{\Sigma}}, \tag{3}$$

where $\bar{\Sigma}$ and s_{Σ} are the mean and standard deviation for the particular set of shear frame tests. Combining the normalized values from the 703 sets gives an aggregate set of 8468 values with mean 0 and standard deviation 0.95. This aggregate set is then partitioned by fracture descriptor so the set of values with a particular fracture descriptor can be compared with the set of 5757 values with planar fractures using a two-tailed *t*-test for unequal sample sizes and unequal variances. Representing the sets of planar and non-planar fracture surfaces with the subscripts 1 and 2, respectively, the calculated value for *t* (Mattson, 1981, p. 430) is

$$t = (\bar{X}_1 - \bar{X}_2) / (s_1^2/n_1 + s_2^2/n_2)^{1/2}, \tag{4}$$

where *X* is the mean, *s* is the standard deviation, *n* is the number of data and the number of degrees of freedom is

$$df = (se_1^2 + se_2^2) / (se_1^4/n_1 + se_2^4/n_2) \tag{5}$$

and the standard error (standard deviation of the mean) is

$$se = \frac{s}{\sqrt{n}}. \tag{6}$$

For each comparison, calculated values of *t* and the total probability associated with both tails, *p*, are shown in Table 4.

Table 6. Effect of frame placement on shear strength measurement

Date/grain form of weak layer	Above weak layer			In weak layer		Difference		t-test for pairs		
	Dist. above	Mean	C. of var.	Mean	C. of var.	Mean	C. of var.	No. of pairs	<i>t</i>	<i>p</i>
	mm	kPa		kPa		kPa				
16 Dec. 1994 rounded facets	10	0.80	0.16	0.46	0.24	-0.33	-0.54	14	6.9	1 × 10 ⁻⁶
29 Jan. 1995 surface hoar	2-5	1.29	0.20	1.04	0.17	-0.26	-0.95	30	5.7	3 × 10 ⁻⁶
23 Jan. 1995 surface hoar	2-5	4.14	0.11	3.65	0.13	-0.49	-1.14	30	4.8	4 × 10 ⁻⁵
29 Jan. 1995 surface hoar	2-5	1.20	0.10	1.06	0.11	-0.15	-1.00	33	5.7	2 × 10 ⁻⁶

Only fracture surfaces with a back divot under the rear compartment >10 mm deep have strength measurements significantly different from planar fractures. Such fractures only occur when the bed surface is not appreciably stronger than the weak layer being tested, typically when both the weak layer and the bed surface consist of facets or depth hoar. For future studies in which minimal variability is important, shear frame tests with such fracture surfaces should be rejected where practical.

TEST SEQUENCE VARIABILITY

P. Schaerer (personal communication, 1991) has suggested that the first shear frame test in a set of tests on a particular weak layer be rejected since the operator requires at least one test to learn the optimal loading rate and frame placement with respect to the weak layer.

To determine if variability is greater for initial tests than for subsequent tests, 703 sets of two or more tests with the standard 0.025 m² frame are used. The strength from each test is normalized using the mean and standard deviation from each set (Equation (3)). The combined set of normalized strengths is then partitioned by sequence number. The means and standard deviations of the set of first tests, set of second tests, etc., and including the set of third to seventh tests are shown in Table 5. Increased variability on the first and second tests in a sequence is apparent in Table 5. The significance of the apparent increase in variability is assessed by comparing the variance of the set of first tests with the variance of the set of third to seventh tests with an *F*-test.

$$F = \left(\frac{s_1}{s_{3-7}} \right)^2. \tag{7}$$

This value of *F* is 1.45, which is significant at the 10⁻⁴ level. Similarly, when the variance of the set of second tests is compared with the variance of the set of third to seventh tests, *F* = 1.14, which is marginally significant (*p* = 0.03). Hence, for future studies in which minimal variability is important, the first and perhaps the second test in a set should be rejected.

FRAME PLACEMENT

When a shear frame is loaded, stress concentrations occur in the snow at the lower edges of the cross-members. Placing the lower edges closer to a weak layer should result in lower strength measurements due to increased stress concentrations in the weak layer. Recommended distances between the bottom edges and the weak layer include “< 5 mm but not through the weak layer” (Perla and Beck, 1983), “just above” (Sommerfeld, 1984) and “a few mm above” (CAA, 1995).

To assess the effect of the distance between the lower edges

Table 7. Effect of different operators on shear strength measurement

Date	Microstructure	Mean load time s	Operator 1	Operator 2	Difference			t-test	
			Mean strength ± S.D. kPa	Mean strength ± S.D. kPa	Mean kPa	Coeff. of var.	Number of pairs	t	p
15 Jan. 1990	Decomp./frag.	1.4	1.10 ± 0.10	1.19 ± 0.23	-0.09	-1.9	7	1.38	0.218
15 Jan. 1990	Graupel	1.7	3.40 ± 0.39	3.01 ± 0.31	0.38	1.6	9	1.87	0.099
31 Jan. 1990	Rounded	1.3	1.69 ± 0.31	1.60 ± 0.22	0.09	3.8	8	0.74	0.485
2 Mar. 1990	Decomp./frag.	1.0	1.64 ± 0.24	1.58 ± 0.18	0.06	4.8	17	0.86	0.403
2 Mar. 1990	Decomp./frag.	1.3	4.12 ± 0.47	3.90 ± 0.50	0.21	1.9	19	2.30	0.034
4 Mar. 1990	Decomp./frag.	0.9	2.23 ± 0.23	2.11 ± 0.28	0.12	2.0	22	2.29	0.032
4 Mar. 1990	Decomp./frag.	1.0	2.07 ± 0.17	2.11 ± 0.28	-0.04	-7.7	22	0.61	0.550
4 Mar. 1990	Decomp./frag.	1.1	2.23 ± 0.23	2.07 ± 0.17	0.16	1.4	22	3.25	0.004
5 Mar. 1990	Rounded	1.0	7.70 ± 0.76	7.22 ± 0.64	0.48	2.3	12	1.54	0.153
5 Mar. 1990	Rounded	1.1	8.04 ± 1.37	7.20 ± 0.67	0.83	1.9	11	1.74	0.112
5 Mar. 1990	Rounded	1.1	8.04 ± 1.37	7.65 ± 0.78	0.39	2.5	11	1.30	0.222
5 Mar. 1990	Rounded	1.0	2.44 ± 0.37	2.52 ± 0.29	-0.08	-4.5	14	0.83	0.420
5 Mar. 1990	Rounded	0.9	2.44 ± 0.37	2.52 ± 0.47	-0.08	-4.0	14	0.93	0.368
5 Mar. 1990	Rounded	0.9	2.52 ± 0.47	2.52 ± 0.29	0.00	134.1	14	0.03	0.978
6 Mar. 1990	Precip. part.	0.6	0.18 ± 0.04	0.19 ± 0.04	-0.01	-7.3	16	0.55	0.591
6 Mar. 1990	Precip. part.	0.5	0.18 ± 0.04	0.18 ± 0.04	0.00	10.7	16	0.38	0.713
6 Mar. 1990	Precip. part.	0.4	0.19 ± 0.04	0.18 ± 0.04	0.01	5.1	16	0.78	0.446
27 Mar. 1990	Rounded	0.6	2.24 ± 0.45	2.24 ± 0.50	0.00	37.0	31	0.02	0.988
30 Mar. 1991	Decomp./frag.	1	0.69 ± 0.07	0.67 ± 0.09	0.01	7.0	31	0.8	0.430
30 Mar. 1991	Decomp./frag.	1	2.03 ± 0.31	2.05 ± 0.20	-0.03	-10.8	27	0.48	0.633

Note: Rows for which $p < 0.05$ are marked in bold.

of the frame and the weak layer, four sets of 14–33 alternating pairs were made during winter 1994/95 with a standard 0.025 m² frame. Each pair consisted of a test with the lower edges placed *in* the weak layer and one with the lower edges placed *above* the weak layer. When the lower edges were placed in the weak layer the strength was reduced by 12%, 13% and 20% compared to strengths obtained with the lower edges 2–5 mm above the weak layer (Table 6). This strength reduction was 41% when the lower edges were placed in the weak layer compared to strengths obtained with the lower edges 10 mm above the weak layer. In every comparison, the strength reduction was significant ($p < 10^{-5}$) based on two-tailed *t*-test for matched pairs.

$$t = \frac{\bar{D}\sqrt{n}}{s_D}, \quad (8)$$

where \bar{D} and s_D are the mean and standard deviation of the differences in strength measurement, respectively.

To reduce stress concentrations, it is clearly advantageous to place the frame above the weak layer. However, this is not always practical since it will sometimes result in a failure within the snow above the weak layer (superstratum). This is most common when the superstratum is comparable in strength to the weak layer. Resulting fracture surfaces may be “wavy” or “irregular”. When failures occur in the snow above the weak layer, usually the only feasible way to test the weak layer is to place the lower edges of the frame in the weak layer.

Fortunately, weak layers of surface hoar commonly result in planar fractures when the shear frame is placed above the weak layer. Occasionally, the superstratum is so hard that it fractures prematurely when the operator pushes the frame into the weak layer. Such “pre-fractures” can sometimes be avoided by pushing the frame only to within

10–20 mm of the weak layer. These “high” placements may result in higher strengths due to reduced stress concentrations in the weak layers or, conceivably, lower strengths due to bending. However, there is no evidence of reduced strength in the one set of shear frames placed 10 mm above the weak layer (Table 6). The sensitivity of shear strength to the distance that the frame is placed above the weak layer represents a limitation of the shear frame test.

Until there are further studies of this effect, we recommend that, whenever practical, the shear frame be placed 2–5 mm above the weak layer, and that whenever snowpack conditions necessitate that the distance between the frame and the weak layer be more or less than the nominal 2–5 mm, the distance should be recorded.

VARIABILITY BETWEEN OPERATORS

The results of shear frame tests can vary between operators because the frame is placed manually and the load is applied manually. Also, operators vary in their ability to locate very thin weak layers, although their skills improve with training and experience.

Operator variability was studied by alternating operators while testing the same layer on the same day. Using the difference in strength measurement between adjacent tests with alternating operators, D , the hypothesis that $D = 0$ is tested with a two-tailed *t*-test (Equation (8)). The results of 20 comparisons are summarized in Table 7 which includes a column for the mean loading time since many of these sets of shear frame tests involve loading times of > 1 s. The hypothesis was rejected at the 1% level ($p < 0.01$) for one comparison involving 22 pairs and for two additional experiments at the 5% level ($p < 0.05$). In the comparison in which a significant difference was detected ($p < 0.01$), one operator was tapping

Table 8. Strength–density regressions by grain form

Grain form (Colbeck and others, 1990)	Number of mean strengths	Density ρ kg m ⁻³	Regression $\Sigma_{\infty} = A(\rho/\rho_{ice})^B$			Regression $\ln \Sigma_{\infty} = A + B \ln(\rho/\rho_{ice})$		
			A	B	R ²	A	B	R ²
Precipitation particles ^a (1)	12	50–110	5.32	1.35	0.42	2.85	1.13	0.31
Graupel (1f)	3	110–235	–	–	–	–	–	–
Decomposed/ fragmented (2)	79	51–270	12.4	1.68	0.56	8.75	1.54	0.47
Rounded grains (3)	16	105–270	8.54	1.26	0.45	7.39	1.20	0.44
Faceted crystals ^b (4)	60	110–330	9.7	1.58	0.41	22.3	2.25	0.58
Rounding facets ^c (4c)	17	195–289	–	–	0.09	–	–	0.10
Depth hoar (5)	10	195–315	–	–	0.12	–	–	–
Group I ^a (1,2,3)	107	50–270	14.5	1.73	0.63	11.6	1.66	0.62
Group II ^b (4,5)	70	110–330	8.5	1.48	0.37	18.5	2.11	0.54

^a Excluding graupel (1f).

^b Excluding rounding facets (4c) and the outlier for faceted crystals with $(\rho, \Sigma_{\infty}) = (285 \text{ kg m}^{-3}, 4.41 \text{ kPa})$.

^c Excludes outlier for rounded facets with $(\rho, \Sigma_{\infty}) = (340 \text{ kg m}^{-3}, 3.50 \text{ kPa})$.

the frame into place with the blade used to cut around the frame while the other was using the standard technique of pushing it into place by hand. When the tapping was discontinued, no significant operator effects ($p > 0.05$) were detected with the first operator. Since the one experiment with $p < 0.01$ can be explained, and marginally significant operator effects ($0.01 < p < 0.05$) occurred in only 2 of 19 experiments, operator effects are not considered to be a source of variability for trained operators and relatively small sets of 7–12 shear frame tests.

SHEAR STRENGTH OF WEAK LAYERS RELATED TO DENSITY

The shear strength of dry snow is strongly related to density (e.g. Keeler and Weeks, 1968; Keeler, 1969; Mellor, 1975; Perla and others, 1982) and grain form (e.g. Keeler and Weeks, 1968; Perla and others, 1982; Föhn, 1993; Föhn and others, 1998).

Perla and others (1982) reported shear strength of snow layers as a function of density, but many density samples included snow from adjacent layers since the weak layers were thinner than their density sampler (20 mm). Föhn (1993) and Föhn and others (1998) reported the shear strength of weak layers and interfaces but did not relate shear strength to density, presumably since many of the weak layers were too thin to be sampled for density. Further, since the failures in weak layers that release slab avalanches are often interfaces (Föhn, 1993), it would seem that density samples of failure layers, and hence a relationship between the shear strength of failure layers and density, are rarely possible. However, for approximately 17% of the failure planes tested with shear frames in the present study, the grains at the failure plane were indistinguishable from an adjacent layer (superstratum or substratum), and the adjacent layer was thick enough ($> 35 \text{ mm}$) for density sampling. The shear strength of these weak planes is related to the density of the indistinguishable adjacent layers in this section. Since surface hoar is always too thin for density sampling and always distinct from adjacent layers, no data for surface hoar are included in Table 8 and Figure 7.

The dependence of tensile and shear strength on density is non-linear (e.g. Keeler and Weeks, 1968; Keeler, 1969; Martinelli, 1971; Mellor, 1975; Perla and others, 1982; Jamieson and Johnston, 1990). Ballard and Feldt's (1965) theoretical

model for sintering of rounded grains is inappropriate since the grains in many of the weak layers in the present study are not rounded and show little evidence of sintering. Also, Perla and others (1982) obtained a better fit to shear strength measurements with the relation

$$\Sigma = A \left(\frac{\rho}{\rho_{ice}} \right)^B, \tag{9}$$

where ρ_{ice} is the density of ice (917 kg m^{-3}) and A and B are empirical constants that depend on grain form.

Since the variance of snow strength increases with the mean strength, Martinelli (1971) and Jamieson and Johnston

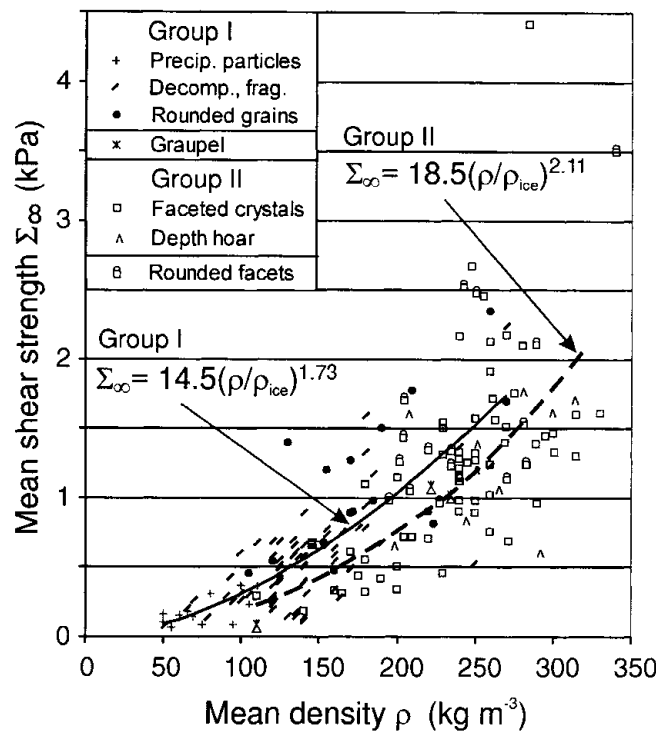


Fig. 7. Shear strength for weak snow layers by density and grain form. Group I consists of precipitation particles, decomposed and fragmented particles and rounded grains but not graupel. Group II consists of faceted crystals and depth hoar but not rounded facets.

(1990) stabilized the variance with a logarithmic transformation of the form

$$\ln \Sigma = \ln A + B \ln \left(\frac{\rho}{\rho_{\text{ice}}} \right). \quad (10)$$

We have adjusted our strength measurements for size effects to obtain Σ_{∞} which is the shear strength of an arbitrarily large specimen (Föhn, 1987b).

For grain-form classes 1–5 (Colbeck and others, 1990), the empirical variables A and B and the coefficients of determination, R^2 , are shown in Table 8 for significant regressions ($p < 0.05$) of shear strength on density with and without the logarithmic transformation. The mean shear strengths are also plotted in Figure 7. Graupel (class 1f) is distinguished from other types of precipitation particles by a different symbol. As reported by a field study of tensile strength (Jamieson and Johnston, 1990), layers of graupel are generally weaker than other types of precipitation particles of similar density. Similarly, Figure 7 uses a different symbol for rounding facets (class 4c) than for other types of facets. Also as shown in Table 8, the 10 mean strengths of depth hoar and the 17 mean strengths of rounding facets are not correlated with density ($p > 0.05$), probably because too few measurements of such layers were obtained.

In the Columbia Mountains where most of the strength measurements were made, precipitation particles (class 1) generally metamorphose into decomposed grains (class 2) which in time metamorphose into rounded grains (class 3). Not surprisingly, these three grain forms show a continuous increase in strength with increasing density, and are assembled as Group I grain forms for additional regressions shown in Table 8. A similar trend for Group I grain forms has also been shown for tensile strength (Jamieson and Johnston, 1990).

Commonly in the Rocky Mountains of western Canada and occasionally in the Columbia Mountains, faceted grains (class 4) metamorphose into depth hoar (class 5). They are assembled into Group II for additional regressions in Table 8. For the regressions of shear strength on density using Equations (9) and (10), the coefficients of determination for the 70 points with Group II grain forms are $R^2 = 0.37$ and $R^2 = 0.54$, respectively. For the 107 points with Group I grain forms, the corresponding coefficients of determination are 0.63 and 0.62. Since the Group II grain forms show reduced coefficients of determination for fewer points, the mean shear strengths are clearly more variable as a function of density. This is consistent with previous studies for tensile strength (Sommerfeld, 1973; Jamieson and Johnston, 1990).

As shown in Table 8, the logarithmic transformation reduces the coefficient of determination for Group I grain forms, and increases it for Group II grain forms. The best fit for Group I grain forms is obtained with the regression based on Equation (9) and with its logarithmic transformation (Equation (10)) for Group II grain forms (Fig. 7).

Based on the regressions in Table 8 and Figure 7, the shear strength of Group II grain forms is 25–50% less than that of Group I grain forms in the density range 125–250 kg m⁻³. This is consistent with field observations that layers of faceted grains are weaker than layers of partly decomposed and/or rounded grains with the same density. We attribute the greater strength for a given density of Group I over Group II to increased bonding associated with equilibrium metamorphism (rounding) which predominates in the evolution of Group I grain forms. Similarly, the strengths of

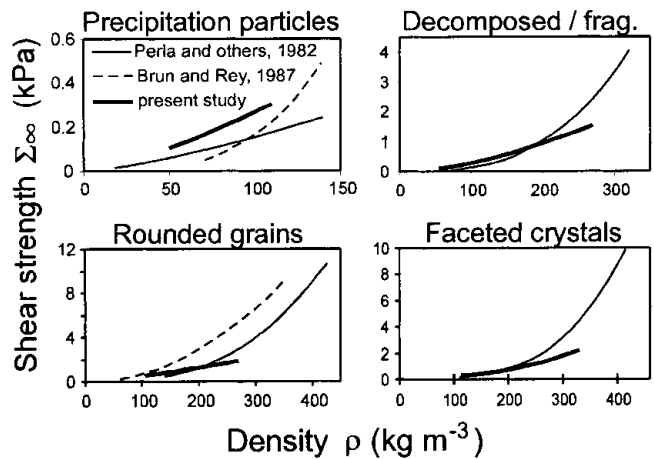


Fig. 8. Comparison of shear strength–density regressions for weak layers from present study with regressions for various layers from Perla and others (1982) and Brun and Rey (1987).

rounded facets fall in the upper part or slightly above the band of strengths for faceted crystals.

The effects of temperature and grain-size on shear strength are not considered in Table 8 or Figure 7. However, after allowing for density effects, Perla and others (1982) report a significant ($p < 0.01$) decrease in strength with increasing grain-size for rounded grains, faceted crystals and melt–freeze grains, and a significant decrease in shear strength with increasing temperature for faceted crystals and melt–freeze grains.

After adjusting for size effects, previous regressions of shear strength on density (Perla and others, 1982; Brun and Rey, 1987) are compared in Figure 8 to the regressions on Equation (9) or (10), whichever has the higher coefficient of determination in Table 8, for precipitation particles, decomposed and fragmented particles, rounded grains and faceted crystals. Many of the data from the previous studies are likely from homogeneous layers and consequently cover wider density ranges than the present study of weak layers. Brun and Rey (1987) provide regressions for “fresh snow” (precipitation particles) and “dry fine grained snow” (rounded grains). For precipitation particles, estimated shear strength from the present study is higher than from the previous studies, but only by 0.05–0.1 kPa. For decomposed and fragmented particles, rounded grains and faceted crystals the estimated shear strength from the present study is lower for higher-density snow and similar to the estimation from the previous studies for lower-density snow.

Maximum normal loads can be estimated from Figure 7. For weak layers with densities of 150 and 250 kg m⁻³, the masses of the snow in the standard 0.025 m² frame are 0.18 and 0.3 kg, respectively, assuming the snow in the frame is 20% denser than the weak layer. Allowing for the 0.2 kg mass of the frame, the maximum normal stresses (on a horizontal weak layer) are 37% and 16% of the corresponding shear strengths for Group II grain forms. Consequently, the shear frame does not measure the “cohesion”, unless normal load effects (Jamieson and Johnston, 1998) are weak.

SUMMARY

Monitoring shear strength of weak layers over time

Since the shear strength of weak layers ranges from 0.1 to at

least 2 kPa (a factor of 20) and the mean of 12 tests has a precision of 10% with 90% confidence, the shear frame test can be used to monitor the change in strength of weak layers over time at fixed locations.

Stress concentrations

There are stress concentrations in the weak layer caused by the load applied to the shear frame cross-members. Cutting along the front and back of the frame, which is necessary to test a known area of the weak layer, causes additional stress concentrations. Placing the frame 2 mm above the weak layer reduces stress concentration according to finite-element analysis.

Frame placement

Placing the bottom of the frame in the weak layer results in lower strengths than obtained by placing the bottom of the frame 2–5 mm or up to 10 mm above the weak layer. Frame placements 2–5 mm above the weak layer usually result in planar fractures, but frames must sometimes be placed in the weak layer or > 5 mm above it to obtain planar fracture surfaces.

Shape of fracture surface

Shear frame tests that result in divots > 10 mm deep under the rear compartment of the frame yield strength measurements significantly greater than tests with planar fractures. No significant effect could be detected for 10 other shapes of fracture surfaces.

Test sequence variability

The first two tests in a set of tests are more variable than subsequent tests and can be rejected to reduce within-set variability.

Different operators

With consistent technique, there is no apparent difference in mean strength measurements obtained by different experienced shear frame operators using the same approximate loading rate and technique for placing the frame.

Distribution of repeated tests

Shear strength measurements from shear frame tests are assumed to be normally distributed since only 4–8 of 28 sets of 30 or more tests show evidence of non-normality.

Variability

Coefficients of variation for shear frame tests average 0.14 and 0.18 from level study plots and avalanche start zones, respectively. These values are less than the 0.25 reported in previous studies, and result in a reduced number of tests to achieve a particular level of precision.

Relationship between shear strength, density and grain form

For a given density of 100–250 kg m⁻³, Group II grain forms (faceted crystals and depth hoar) have substantially lower shear strength than Group I grain forms (precipitation particles, decomposed and fragmented particles, and rounded grains). The regressions in Table 8 can be used to

estimate the shear strength for some common grain forms of weak snowpack layers.

ACKNOWLEDGEMENTS

For financial support we are grateful to the BC Helicopter and Snowcat Skiing Operators Association, the Natural Sciences and Engineering Research Council of Canada, Canadian Mountain Holidays, Mike Wiegele Helicopter Skiing, Canada West Ski Areas Association, Intrawest Corporation and the Canadian Avalanche Association.

For their expertise and fieldwork, we thank M. Shubin, J. Hughes, L. Allison, K. Black, J. Blench, A. Cooperman, M. Gagnon, T. Geldsetzer, S. Gould, B. Gould, B. Johnson, G. Johnson, A. Jones, P. Langevin, G. McAuley, R. McGowan and A. Wilson. We are grateful to J. Lockhart for proofreading the paper, and to J. Hughes, P. Schaerer, R. Perla, C. Stethem, J. Schweizer and P. Föhn for helpful discussions on shear frame testing.

REFERENCES

- Ballard, G. E. H. and E. D. Feldt. 1965. Considerations of the strength of snow. *CRREL Res. Rep.* 184.
- Brun, E. and L. Rey. 1987. Field study on snow mechanical properties with special regard to liquid water content. *International Association of Hydrological Sciences Publication* 162 (Symposium at Davos 1986 — *Avalanche Formation, Movement and Effects*), 183–192.
- Canadian Avalanche Association (CAA). 1995. *Observation guidelines and recording standards for weather, snowpack and avalanches*. Revelstoke, B.C., Canadian Avalanche Association.
- Colbeck, S. C. and 7 others. 1990. *The international classification for seasonal snow on the ground*. Wallingford, Oxon, International Association of Scientific Hydrology. International Commission on Snow and Ice.
- Daniels, H. E. 1945. The statistical theory of the strength of bundles of threads. *Proc. R. Soc. London, Ser. A*, **183**(995), 405–435.
- De Quervain, M. 1951. Strength properties of a snow cover and its measurement [Die Festigkeitseigenschaften der Schneedecke und ihre Messung]. *SIPRE Transl.* 9.
- Föhn, P. M. B. 1987a. The “Rutschblock” as a practical tool for slope stability evaluation. *International Association of Hydrological Sciences Publication* 162 (Symposium at Davos 1986 — *Avalanche Formation, Movement and Effects*), 223–228.
- Föhn, P. M. B. 1987b. The stability index and various triggering mechanisms. *International Association of Hydrological Sciences Publication* 162 (Symposium at Davos 1986 — *Avalanche Formation, Movement and Effects*), 195–214.
- Föhn, P. M. B. 1993. Characteristics of weak snow layers or interfaces. In Armstrong, R., ed. *ISSW '92. A merging of theory and practice. International Snow Science Workshop, 4–8 October 1992, Breckenridge, Colorado. Proceedings*. Denver, CO, Avalanche Information Center, 160–170.
- Föhn, P. and C. Camponovo. 1997. Improvements by measuring shear strength of weak layers. In *ISSW '96. International Snow Science Workshop, 6–10 October 1996, Banff, Alberta. Proceedings*. Revelstoke, B.C., Canadian Avalanche Association, 158–162.
- Föhn, P. M. B., C. Camponovo and G. Krüsi. 1998. Mechanical and structural properties of weak snow layers measured in situ. *Ann. Glaciol.*, **26**, 1–6.
- Fukuzawa, T. and H. Narita. 1993. An experimental study on mechanical behavior of a depth hoar under shear stress. In Armstrong, R., ed. *ISSW '92. A merging of theory and practice. International Snow Science Workshop, 4–8 October 1992, Breckenridge, Colorado. Proceedings*. Denver, CO, Avalanche Information Center, 171–175.
- Gubler, H. 1978. An alternate statistical interpretation of the strength of snow. *J. Glaciol.*, **20**(83), 343–357.
- Jamieson, J. B. 1989. *In situ* tensile strength of snow in relation to slab avalanches. (M.Sc. thesis, University of Calgary. Department of Civil Engineering.)
- Jamieson, J. B. 1995. *Avalanche prediction for persistent snow slabs*. (Ph.D. thesis, University of Calgary.)
- Jamieson, J. B. and C. D. Johnston. 1990. *In-situ* tensile tests of snow-pack layers. *J. Glaciol.*, **36**(122), 102–106.
- Jamieson, J. B. and C. D. Johnston. 1998. Refinements to the stability index for skier-triggered dry-slab avalanches. *Ann. Glaciol.*, **26**, 296–302.
- Keeler, C. M. 1969. The growth of bonds and the increase of mechanical

- strength in a dry seasonal snow-pack. *J. Glaciol.*, **8**(54), 441–450.
- Keeler, C. M. and W. F. Weeks. 1968. Investigations into the mechanical properties of alpine snow-packs. *J. Glaciol.*, **7**(50), 253–271.
- Martinelli, M., Jr. 1971. Physical properties of alpine snow as related to weather and avalanche conditions. *U.S. For. Serv. Res. Pap.* RM-64.
- Mattson, D. E. 1981. *Statistics: difficult concepts, understandable explanations*. St Louis, MO, Mosby.
- Mellor, M. 1975. A review of basic snow mechanics. *International Association of Hydrological Sciences Publication* 114 (Symposium at Grindelwald 1974 — *Snow Mechanics*), 251–291.
- Narita, H. 1980. Mechanical behaviour and structure of snow under uniaxial tensile stress. *J. Glaciol.*, **26**(94), 275–282.
- Perla, R. 1977. Slab avalanche measurements. *Can. Geotech. J.*, **14**(2), 206–213.
- Perla, R. and T. M. H. Beck. 1983. Experience with shear frames. *J. Glaciol.*, **29**(103), 485–491.
- Perla, R., T. M. H. Beck and T. T. Cheng. 1982. The shear strength index of alpine snow. *Cold Reg. Sci. Technol.*, **6**(1), 11–20.
- Roch, A. 1966a. Les déclenchements d'avalanches. *International Association of Scientific Hydrology Publication* 69 (Symposium at Davos 1965 — *Scientific Aspects of Snow and Ice Avalanches*), 182–195.
- Roch, A. 1966b. Les variations de la résistance de la neige. *International Association of Scientific Hydrology Publication* 69 (Symposium at Davos 1965 — *Scientific Aspects of Snow and Ice Avalanches*), 86–99.
- Schleiss, V. G. and W. E. Schleiss. 1970. Avalanche hazard evaluation and forecast, Rogers Pass, Glacier National Park. In Gold, L. W. and G. P. Williams, eds. *Ice engineering and avalanche forecasting*. Ottawa, Ont., National Research Council of Canada. Associate Committee on Geotechnical Research, 115–122. (ACGR Tech. Mem. 98.)
- Singh, H. 1980. A finite-element model for the prediction of dry slab avalanches. (Ph.D. thesis, Colorado State University)
- Sommerfeld, R. A. 1973. Statistical problems in snow mechanics. *U.S. For. Serv. Gen. Tech. Rep.* RM-3, 29–36.
- Sommerfeld, R. A. 1980. Statistical models of snow strength. *J. Glaciol.*, **26**(94), 217–223.
- Sommerfeld, R. A. 1984. Instructions for using the 250 cm² shear frame to evaluate the strength of a buried snow surface. *U.S. For. Serv. Res. Note* RM-446, 1–6.
- Sommerfeld, R. A. and R. M. King. 1979. A recommendation for the application of the Roch index for slab avalanche release. *J. Glaciol.*, **22**(88), 547–549.
- Sommerfeld, R. A., R. M. King and F. Budding. 1976. A correction factor for Roch's stability index of slab avalanche release. *J. Glaciol.*, **17**(75), 145–147.
- Statsoft. 1994. *Statistica Volume I: general conventions and statistics I*. Tulsa, OK, Statsoft.